Handheld forward-imaging needle endoscope for ophthalmic optical coherence tomography inspection

Shuo Han,[a] Marinko V. Sarunic,[c] Jigang Wu,[a] Mark Humayun,[d] and Changhuei Yang[a,b,*]
[a]California Institute of Technology, Department of Electrical Engineering (MC 136-93)
[b]Department of Bioengineering (MC 138-78), Pasadena, California 91125
[c]Simon Fraser University, School of Engineering Science,Burnaby, BC, Canada V5A 1S6
[d]University of Southern California, Doheny Eye Institute, Los Angeles, California 90033

Abstract. We report the narrowest to-date (21 gauge, 820-μm-diam) handheld forward-imaging optical coherence tomography (OCT) needle endoscope and demonstrate its feasibility for ophthalmic OCT inspection. The probe design is based on paired-angle-rotation scanning (PARS), which enables a linear B-scan pattern in front of the probe tip by using two counterrotating angle polished gradient-index (GRIN) lenses. Despite its small size, the probe can provide a numerical apertune (NA) of 0.22 and an experimental sensitivity of 92 dB at 0.5 frame/s. The feasibility of retinal imaging is tested on enucleated *ex vivo* porcine eyes, where structural features including remnant vitreous humor, retina, and choroid can be clearly distinguished. Due to its imaging quality comparable to a commercial OCT system and compatibility with the current ophthalmic surgery standard, the probe can potentially serve as a better alternative to traditional visual inspection by white light illumination during vitreoretinal surgery (e.g., vitrectomy). [DOI: 10.1117/1.2904664]

Keywords: optical coherence tomography; endoscopic imaging; retina scanning.

Paper 07354LRR received Aug. 28, 2007; revised manuscript received Feb. 1, 2008; accepted for publication Feb. 3, 2008; published online Apr. 21, 2008.

Since its invention in the 1990s, optical coherence tomography (OCT) has generated wide interest as a biomedical imaging modality due to its noninvasive nature and high resolution imaging capability.[1] However, scattering and/or absorption of tissue to near-IR light permits only millimeter scale penetration depth, thus limiting the use of OCT in deep-tissue imaging. One way to circumvent this is by incorporating OCT into an endoscopic needle probe. OCT endoscopes are capable of penetrating deep into tissues where structural information can then be collected by internal optical elements. In general, OCT needle endoscopes fall into two categories based on their region of inspection: side imaging[2–5] and forward imaging.[6–8] The former probe type typically has a relatively simpler structure and is amenable to miniaturization—a probe diameter of 410 μm has been reported.[3] Forward-imaging probes are generally more complicated in their optical designs and actuation mechanisms. Despite their relative complexities, these probes are being actively developed as they are well suited to provide guidance and real-time monitoring during surgeries.

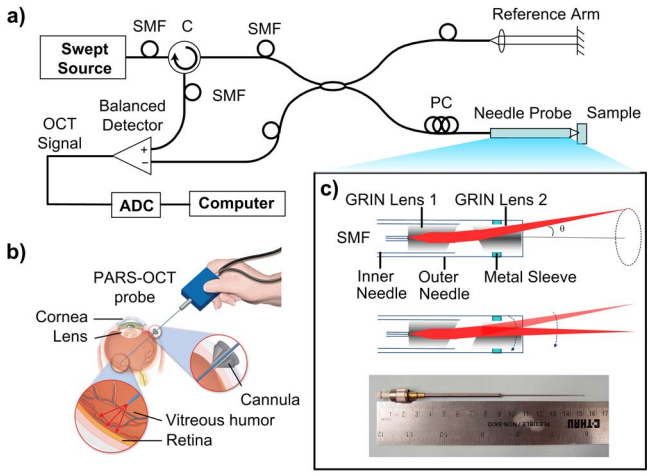

Fig. 1 (a) Swept source OCT setup with PARS-OCT probe; (b) schematic of the application of PARS-OCT probe during vitrectomy, a surgical procedure for removal of vitreous humor; and (c) photograph of PARS-OCT probe and its beam-steering principle (SMF: single-mode fiber; ADC: analog-digital converter).

One potential application of an OCT forward-imaging probe is in aiding vitrectomy,[9] which is a surgical procedure to remove the vitreous humor, as sketched in Fig. 1. Vitrectomy is a required precursor to other surgeries for the treatment of severe eye diseases such as retinal detachment. The success of the procedure and the long-term prognosis for patients depend critically on the complete removal of vitreous humor around retinal tears and holes. To guarantee this, surgeons will typically insert a light pipe through an incision on the patient's eye and examine the remnant vitreous by direct illumination during eye surgery. As the vitreous is clear, this examination is often difficult. OCT can aid in this procedure by providing depth-resolved images without the introduction of a contrast agent. Compared to commercial slit-lamp-based OCT, a forward-imaging OCT endoscopic probe can be brought in close proximity to the retinal surface, avoiding the necessity of imaging through the cornea and crystalline lens. To minimize the damage due to incision, a small-diameter probe is highly desirable. The endoscope design using paired-angle-rotation scanning (PARS) developed by our group[10] is well suited for this purpose because it offers a large scanning range and excellent scalability.

In this letter, we report on our successful implementation of a 21-gauge (820-μm-diam) PARS-OCT forward-imaging needle probe, and demonstrate its use by collecting OCT images from enucleated *ex vivo* porcine eyes. To our knowledge, this is the narrowest forward-imaging OCT probe that has yet been reported. The narrow probe can easily fit through the standard cannula or scleral incisions employed in ophthalmic

*E-mail: chyang@caltech.edu, Tel: 1-626-395-8922, Fax: 1-626-395-8475

1083-3668/2008/13(2)/020505/3/$25.00 © 2008 SPIE

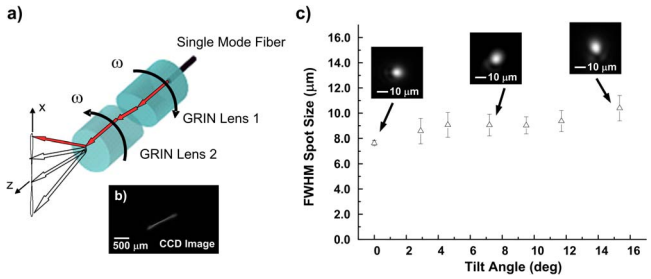

Fig. 2 (a) Planar sweep pattern achieved when the two GRIN lenses rotated with equal and opposite velocities, (b) scan pattern as recorded by a CCD camera placed 2 mm from the probe tip, and (c) measured spot size (FWHM) versus tilt angle. The spot profile is also shown for selected tilt angles.

surgery. Furthermore, the probe and its redesigned actuation system are suitably compact and lightweight for handheld use by a surgeon.

The PARS-OCT probe design utilizes two angle-polished gradient-index (GRIN) lenses [d=500 μm, numerical apertune (NA)=0.22], which are rotated about the optical axis to steer the optical beam position.[10] As sketched in Fig. 1, the GRIN lenses are encased in two counterrotating concentric needles (23 gauge/21 gauge for the inner/outer needle). Fabrication of the angle-cut GRIN lenses and their placements in the needles were performed by GRINTECH GmbH. The inner faces of both GRIN lenses are polished at a 15 deg angle, and separated by a designed air gap. Refraction at the first angle-polished surface directs the beam off axis to the second GRIN lens, providing a maximum tilt angle of 15.3 deg. The first GRIN lens is $\frac{1}{4}$ pitch (l=3.11 mm). The second GRIN lens is less than $\frac{1}{4}$ pitch (l=2.6 mm). The working distance of the probe was measured to be 0.78 ± 0.02 mm. Controlling the angle of the GRIN lenses with respect to each other determines the scan pattern. Due to the watery nature of vitreous humor, the gap between the GRIN lenses and needle tubing was sealed using epoxy to prevent fluid contamination. During use, all the elements were mounted onto a dedicated chassis built from commercially available cage systems. To avoid complicated control electronics and for better stability, both needles were driven together by one single lightweight dc motor and associated bevel gears to ensure the same rotational speed in opposite directions, providing a planar sweep scan. The scan confinement can be seen from Fig. 2, which was recorded by suspending the scanning PARS-OCT probe tip above a planar CCD camera at a distance of 2 mm. This scan system has an additional advantage—the scanning simply requires the motor to maintain a constant rotational speed, and does not require well-timed acceleration or deceleration. We plotted the motor's integrated encoder output as a function of time and found that speed deviation was insignificant (a correlation fit of r=0.99995).

The PARS-OCT probe design is compatible with any center optical wavelength; in this case, we designed the prototype for operation at 1310 nm, as opposed to ~800 nm, which is the typical wavelength for OCT retinal imaging. A central wavelength of 1310 nm is desirable as we can expect to achieve improved visibility of the choroid and choriocapillaries over the more common shorter wavelengths.[11] An additional benefit of using 1310-nm illumination with the PARS-OCT probe is that its higher absorption in vitreous can be expected to improve visualization of remnant vitreous adhering to the retina. Capitalizing on the inherent sensitivity advantage of Fourier domain systems,[12–14] a commercially available swept laser was selected as the source illumination (Micron Optics, λ_o=1310 nm, $\Delta\lambda$=70 nm, 250-Hz A-scan rate). A resampling algorithm[15] was used, where the k-domain sampling clock signal was generated by a fiber Fabry-Pérot interferometer.

The PARS-OCT probe requires beam propagation through GRIN lenses, which could potentially introduce significant image artifact. In particular, chromatically based aberrations were anticipated due to the use of a spectrally broad source. Additionally, an off-axis aberration unique to the PARS-OCT probe can occur due to the dispersive effects of the internal angle-polished surfaces. This can potentially introduce a broadening of the focal spot with increasing scan angle, and was a major design concern during the probe design process. We measured the focal spot size of our prototype at different tilt angles by projecting the focal spot onto a CCD camera through a 20X objective combined with an achromat doublet. We found that the minimum spot size of 7.6 μm (FWHM) was obtained when the beam exited the probe with no tilt. The spot size increased moderately to 10.4 μm (26.4% increase) at the maximum tilt angle. The trend is consistent with our ZEMAX simulations, which showed a spot size of 5.0 μm at no tilt and an increase of 31.5% at maximum tilt. The spot size discrepancy between the simulations and the probe prototype can be attributed to two major reasons. First, the ZEMAX simulations for GRIN lenses assumed paraxial propagation and, as such, oversimplified the actual beam propagation, which involves significant angular light deflection between the two GRIN lenses. This implies that the ZEMAX simulations can be expected to underestimate the spot size. Second, the spacing (~50 μm) between the two GRIN lenses was difficult to control during the probe fabrication process. For these two reasons, we expect the ZEMAX simulations to be useful as a guide but not as a fit to the experimentally measured spot size. We also measured the depth of focus to be 0.26 ± 0.03 mm and it was insensitive to the tilt angle (within the error limit). Finally, we quantified the influence of unmatched dispersion by comparing the axial resolutions of the OCT system with and without the probe inserted, which are 10.5 ± 0.1 and 7.8 ± 0.1 μm, respectively. We found that the resolution was not sensitive to the tilt angle; this was anticipated as the fractional change in optical path length through the GRIN lenses as a function of tilt angle is small (~1.3%).

For a preliminary test on its feasibility in clinical application, the PARS-OCT probe was used to image the retina of an enucleated porcine eye with cornea, lens, and vitreous removed. The power delivered at the sample was about 0.6 mW, and balanced detection was used. The experimental system sensitivity was measured to be 92 dB, which is 15 dB less than that with a free-space sample arm, consistent with the measured insertion loss introduced by the PARS probe (7.5 dB one way, 15 dB round-trip). During imaging, we collected several B-scans, which consisted of 500 A-scans each at a B-scan rate of 0.5 frames/s. We then converted the data to a sonogram-like image to account for the fan scan pattern.

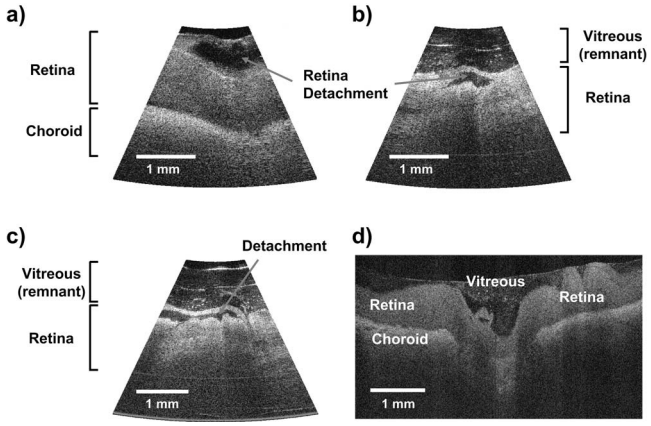

Fig. 3 (a), (b), and (c) Porcine retinal images acquired by PARS-OCT probe. The retina layer was partially detached during the removal of vitreous humor. Some remnants of vitreous on the retina were still visible. (d) Retinal image from a commercial OCT microscope.

In the resulting images, shown in Fig. 3, structures as deep as ~2.5 mm from the probe tip were clearly observed, including top remnant vitreous, retina, and choroid underneath the retina layer. In several places, we were also able to observe the detachments of the retina from the choroid, which likely occurred during removal of the vitreous humor. An image of the enucleated retina after lensectomy and vitrectomy captured by a commercial 1310-nm OCT microscope (Thorlabs OCM1300SS) is also shown for comparison. The images acquired with the PARS-OCT probe are seen to have comparable quality to that acquired with the commercial system. A faster B-scan rate can be achieved by either switching to a higher line rate OCT engine or by reducing the number of A-scans in each B-scan image. A large increase in scan rate may also require better actuation system designs and tighter design tolerances to prevent undesirable probe vibrations. With our current system, probe vibrations appeared to be minimal but they may be contributive to some of the vertical speckle smear in the images in Fig. 3. Finally, note that the rotation of the outer needle probe did not cause any observable tears in the sample. In applications where the probe must make contact with stiff tissue types, we may need to sheath the probe in a nonrotating needle to avoid frictional artifacts.

In conclusion, we successfully fabricated a miniaturized PARS-OCT probe that was suitable for endoscopic inspection. The probe featured a 21-gauge outer diameter and was compatible with current ophthalmic surgical procedures. Retinal images were captured using this PARS-OCT probe combined with a swept-source OCT system that ran at 0.5 frame/s. Images with quality comparable to commercial OCT microscope were acquired; we can clearly see interesting features, including remnant vitreous, retina, and choroid, in the images. This endoscope design can potentially help resolve the difficulty in direct visual inspection during surgery procedures such as vitrectomy.

Acknowledgments

The authors would like to thank Jian Ren for helpful discussions and Caltech chemistry machine shop for fabricating the probe chassis. This work was funded by Biomimetic MicroElectronic Systems Engineering Research Center (BMES ERC, No. EEC-0310723), a National Science Foundation (NSF) Career Award (No. BES-0547657), and the Caltech Grubstake fund.

References

1. D. Huang, E. A. Swanson, C. P. Lin, J. S. Schuman, W. G. Stinson, W. Chang, M. R. Hee, T. Flotte, K. Gregory, C. A. Puliafito, and J. G. Fujimoto, "Optical coherence tomography," *Science* **254**, 1178–1181 (1991).
2. G. J. Tearney, S. A. Boppart, B. E. Bouma, M. E. Brezinski, N. J. Weissman, J. F. Southern, and J. G. Fujimoto, "Scanning single-mode fiber optic catheter-endoscope for optical coherence tomography," *Opt. Lett.* **21**, 543–545 (1996).
3. X. Li, C. Chudoba, T. Ko, C. Pitris, and J. G. Fujimoto, "Imaging needle for optical coherence tomography," *Opt. Lett.* **25**, 1520–1522 (2000).
4. P. R. Herz, Y. Chen, A. D. Aguirre, K. Schneider, P. Hsiung, J. G. Fujimoto, K. Madden, J. Schmitt, J. Goodnow, and C. Petersen, "Micromotor endoscope catheter for *in vivo*, ultrahigh-resolution optical coherence tomography," *Opt. Lett.* **29**, 2261–2263 (2004).
5. J. Su, J. Zhang, L. Yu, and Z. Chen, "*In vivo* three-dimensional microelectromechanical endoscopic swept source optical coherence tomography," *Opt. Express* **15**, 10390–10396 (2007).
6. T. Xie, H. Xie, G. K. Fedder, and Y. Pan, "Endoscopic optical coherence tomography with a modified microelectromechanical systems mirror for detection of bladder cancers," *Appl. Opt.* **42**, 6422–6426 (2003).
7. X. Liu, M. J. Cobb, Y. Chen, M. B. Kimmey, and X. Li, "Rapid-scanning forward-imaging miniature endoscope for real-time optical coherence tomography," *Opt. Lett.* **29**, 1763–1765 (2004).
8. T. Xie, S. Guo, Z. Chen, D. Mukai, and M. Brenner, "GRIN lens rod based probe for endoscopic spectral domain optical coherence tomography with fast dynamic focus tracking," *Opt. Express* **14**, 3238–3246 (2006).
9. R. Machemer, "The development of pars plana vitrectomy: a personal account," *Graefe's Arch. Clin. Exp. Ophthalmol.* **233**, 453–468 (1995).
10. J. Wu, M. Conry, C. Gu, F. Wang, Z. Yaqoob, and C. Yang, "Paired-angle-rotation scanning optical coherence tomography forward-imaging probe," *Opt. Lett.* **31**, 1265–1267 (2006).
11. B. Povazay, K. Bizheva, B. Hermann, A. Unterhuber, H. Sattmann, A. Fercher, W. Drexler, C. Schubert, P. Ahnelt, M. Mei, R. Holzwarth, W. Wadsworth, J. Knight, and P. S. J. Russell, "Enhanced visualization of choroidal vessels using ultrahigh resolution ophthalmic OCT at 1050 nm," *Opt. Express* **11**, 1980–1986 (2003).
12. M. A. Choma, M. V. Sarunic, C. Yang, and J. Izatt, "Sensitivity advantage of swept source and Fourier domain optical coherence tomography," *Opt. Express* **11**, 2183–2189 (2003).
13. J. F. de Boer, B. Cense, B. H. Park, M. C. Pierce, G. J. Tearney, and B. E. Bouma, "Improved signal-to-noise ratio in spectral-domain compared with time-domain optical coherence tomography," *Opt. Lett.* **28**, 2067–2069 (2003).
14. R. Leitgeb, C. K. Hitzenberger, and A. F. Fercher, "Performance of Fourier domain vs. time domain optical coherence tomography," *Opt. Express* **11**, 889–894 (2003).
15. R. Huber, M. Wojtkowski, K. Taira, J. Fujimoto, and K. Hsu, "Amplified, frequency swept lasers for frequency domain reflectometry and OCT imaging: design and scaling principles," *Opt. Express* **13**, 3513–3528 (2005).